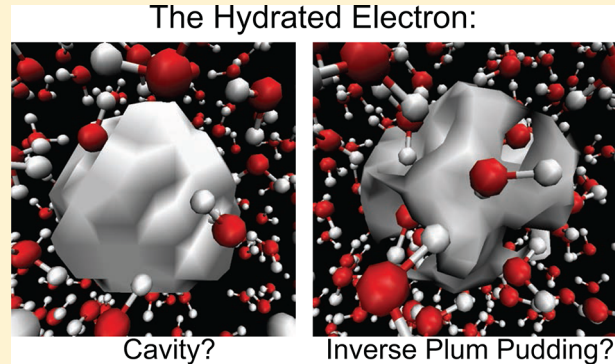


# To Be or Not to Be in a Cavity: The Hydrated Electron Dilemma

Jennifer R. Casey, Argyris Kahros, and Benjamin J. Schwartz\*

Department of Chemistry and Biochemistry, University of California, Los Angeles, Los Angeles, California 90095-1569, United States

**ABSTRACT:** The hydrated electron—the species that results from the addition of a single excess electron to liquid water—has been the focus of much interest both because of its role in radiation chemistry and other chemical reactions, and because it provides for a deceptively simple system that can serve as a means to confront the predictions of quantum molecular dynamics simulations with experiment. Despite all this interest, there is still considerable debate over the molecular structure of the hydrated electron: does it occupy a cavity, have a significant number of interior water molecules, or have a structure somewhere in between? The reason for all this debate is that different computer simulations have produced each of these different structures, yet the predicted properties for these different structures are still in reasonable agreement with experiment. In this Feature Article, we explore the reasons underlying why different structures are produced when different pseudopotentials are used in quantum simulations of the hydrated electron. We also show that essentially all the different models for the hydrated electron, including those from fully *ab initio* calculations, have relatively little direct overlap of the electron's wave function with the nearby water molecules. Thus, a non-cavity hydrated electron is better thought of as an “inverse plum pudding” model, with interior waters that locally expel the surrounding electron's charge density. Finally, we also explore the agreement between different hydrated electron models and certain key experiments, such as resonance Raman spectroscopy and the temperature dependence and degree of homogeneous broadening of the optical absorption spectrum, in order to distinguish between the different simulated structures. Taken together, we conclude that the hydrated electron likely has a significant number of interior water molecules.



## ■ INTRODUCTION: THE STRUCTURE OF THE HYDRATED ELECTRON

The hydrated electron, which is a single excess electron in electrically neutral liquid water, is an important chemical species in areas of science ranging from biological processes to radiation chemistry. However, despite years of intense study using both theoretical and experimental techniques,<sup>1</sup> there is still not universal consensus on the molecular structure of this simplest of quantum mechanical solutes. The theoretical methods most commonly used to model the hydrated electron involve mixed quantum/classical (MQC) simulations, where the excess electron is treated quantum mechanically and the surrounding water molecules are treated classically. One of the key features of the one-electron approximation inherent in MQC approaches to study the hydrated electron is the use of an electron–water pseudopotential. As we discuss further below, it turns out that the molecular structure of the hydrated electron obtained from MQC simulations is extremely sensitive to the choice of this pseudopotential—the sensitivity is so high that small changes in the functional form of the potential can literally turn the hydrated electron's molecular structure inside out. Since experiments have not been able to conclusively determine a structure for the hydrated electron, in this Feature Article, we explore the questions of what exactly the hydrated electron looks like and how physically reasonable are the various proposed structures.

Instinctively, one would expect the hydrated electron to be repelled by each of the surrounding water molecules; after all, the Pauli exclusion principle tells us that the excess electron cannot occupy the same regions of space that are already occupied by the electrons residing in the water molecules' molecular orbitals (MOs). On the basis of this idea, the early picture that emerged was that of a hydrated electron which expelled the nearby solvent molecules and occupied a cavity in the water.<sup>2</sup> From this perspective, the hydrated electron is expected to act like an aqueous halide, midway in size between chloride and bromide,<sup>3</sup> but with a structure that is softer and more flexible than that of the halides due to the highly polarizable nature of the electron. This cavity picture was reinforced by early MQC simulation studies.<sup>4,5</sup> For example, Schnitker and Rossky (SR), who used a pseudopotential that was later found to contain an error,<sup>6</sup> performed MQC simulations that indicated that the hydrated electron resides in a cavity that is surrounded by six bond-oriented water molecules.<sup>3,7,8</sup> This structure, which is shown in Figure 1a, was quite reminiscent of the structure suggested in earlier EPR experiments performed on excess electrons in aqueous alkaline glassy matrixes.<sup>9</sup> Later, Turi, Borgis, and their

**Received:** August 7, 2013

**Revised:** September 6, 2013

**Published:** October 4, 2013

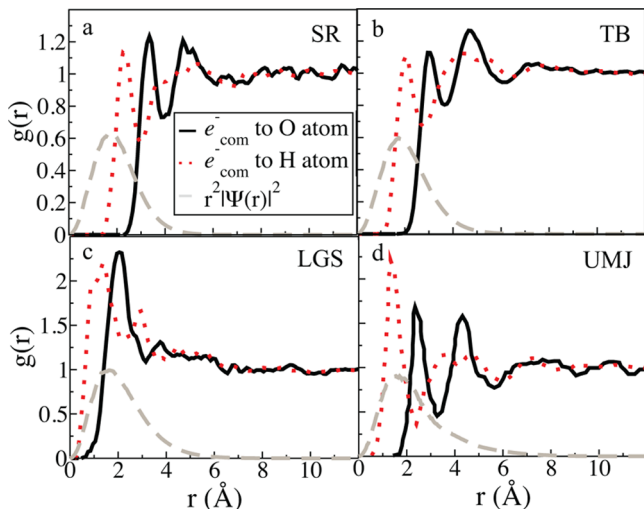


**Figure 1.** The radial distribution functions of the electron center of mass to water O atoms (black, full) and H atoms (red, dotted), along with the electron density (gray, dashed) for the (a) SR, (b) TB, (c) LGS, and (d) UMJ models. The SR and TB models show a clear cavity occupied by the electron, while no cavity is present in the LGS model and only a very small cavity is present in the UMJ model.

co-workers (TB) ran MQC molecular dynamics (MD) simulations that also suggested that the hydrated electron occupied a cavity in the water, although the particular structure (with only roughly four first-shell water molecules, Figure 1b) was different than that suggested by SR.<sup>10,11</sup> More recently, the effects of dynamic water polarization on the hydrated electron's structure and energetics were explored by Jacobson and Herbert.<sup>12,13</sup> Although electronic polarization is included in most hydrated electron models in a mean-field manner,<sup>14</sup> Jacobson and Herbert extended the TB model to treat the water polarization explicitly and self-consistently. These authors found that the explicit inclusion of water polarizability is important both in obtaining meaningful ionization potentials and in correctly capturing the blue tail of the optical absorption spectra. However, these authors also observed that including polarizability only slightly modified the structure of the hydrated electron from that seen by TB: even with polarizability, the hydrated electron still resides in a cavity (albeit a slightly smaller one than seen without self-consistent polarizability) surrounded by approximately four first-shell water molecules. Finally, recent MQC simulations performed by Larsen, Glover, and Schwartz (LGS) have suggested a completely different picture for the hydrated electron; rather than dwelling in a cavity, LGS suggested that the hydrated electron occupies a region of enhanced water density ( $\rho \approx 1.2 \text{ g/cm}^3$ ), with many water molecules residing in the interior of the excess electron's charge density (Figure 1c).<sup>15</sup>

## ■ CONTROVERSY OVER HYDRATED ELECTRON MD SIMULATIONS

Even though the calculated properties of the LGS non-cavity hydrated electron agreed as well with experiment as predictions from cavity models,<sup>15–17</sup> the idea of a hydrated electron with interior waters quickly met with significant resistance.<sup>18–20</sup> This lack of acceptance for a non-cavity electron partially stems from the fact that the calculated

properties of the hydrated electron depend sensitively on the nature of the pseudopotential chosen for the simulation. Both TB and LGS derived their pseudopotentials from the Phillips–Kleinman (PK) formalism, which provides a prescription for calculating a potential that guarantees that the wave function of the excess electron is orthogonal to the wave functions of all the electrons in the water MOs (as calculated at the Hartree–Fock level of theory).<sup>21,22</sup> Even though they are constructed for use in the condensed phase, it is important to note that these pseudopotentials are based on the quantum chemistry of an excess electron interacting with a single, gas-phase molecule. A single, gas-phase water molecule, however, does not bind an excess electron. Thus, when constructing such pseudopotentials, it is typical to alter the quantum chemistry of the isolated water molecule either by adding a confinement potential to hold the excess electron in the vicinity of the water molecule or by implementing a basis set with finite range. It is expected that these types of approximations only alter the calculated potential at long range, so that the short-range part that is most important for condensed-phase simulation is robust, but we are not aware of any detailed exploration of the full effects of these approximations in the literature.

Regardless of the details behind the development of a PK pseudopotential, it is not computationally feasible to use the full numerical PK potential in a MQC simulation; the standard procedure has been to fit this potential with an analytic function. TB decided to fit the numerically determined PK pseudoorbital with a very simple function. They adjusted the parameters of their fit to guarantee that the eigenenergy would be correct, but the functional form they chose missed many of the physical features which determine the pseudopotential. For example, the full, exact PK potential for an excess electron interacting with a water molecule has an attractive region behind the water O atom (opposite the H atoms) and a strongly repulsive region between the H atoms (Figure 2a) that are missed by the TB fit (cf. Figure 2e). LGS, on the other hand, decided to fit this same PK pseudopotential in such a way as to retain these distinct features but at the cost of changing the eigenenergy by  $\sim 0.1$  eV (Figure 2b). Perhaps even more surprising, small changes in the shape of the fitting function can change the behavior of the simulated hydrated electron from cavity to non-cavity or back again.<sup>16,18</sup> Thus, starting with an identical formalism, TB and LGS have produced two very different pictures of the hydrated electron, all because of subtle details in the way that the numerical PK pseudoorbital and pseudopotential were analytically fit.

Another issue with the implementation of pseudopotentials in hydrated electron simulations is the fact that such potentials have strongly varying features on length scales short compared to the water O–H bond. This means that the basis sets in simulations using such potentials must be extensive enough to capture spatial variation in the wave function on the same length scale as the variations in the potential. Since it is impractical to use more than  $\sim 10^4$  basis functions in dynamical simulations (as would be required to calculate the hydrated electron's wave function both on top of and between the water molecules), the standard practice is to spatially smooth the potential to remove the finer features.<sup>10,15</sup> Figure 2 also shows plots of the numerically exact PK pseudopotential after having been smoothed (via convolution of the PK pseudoorbital with a Gaussian before

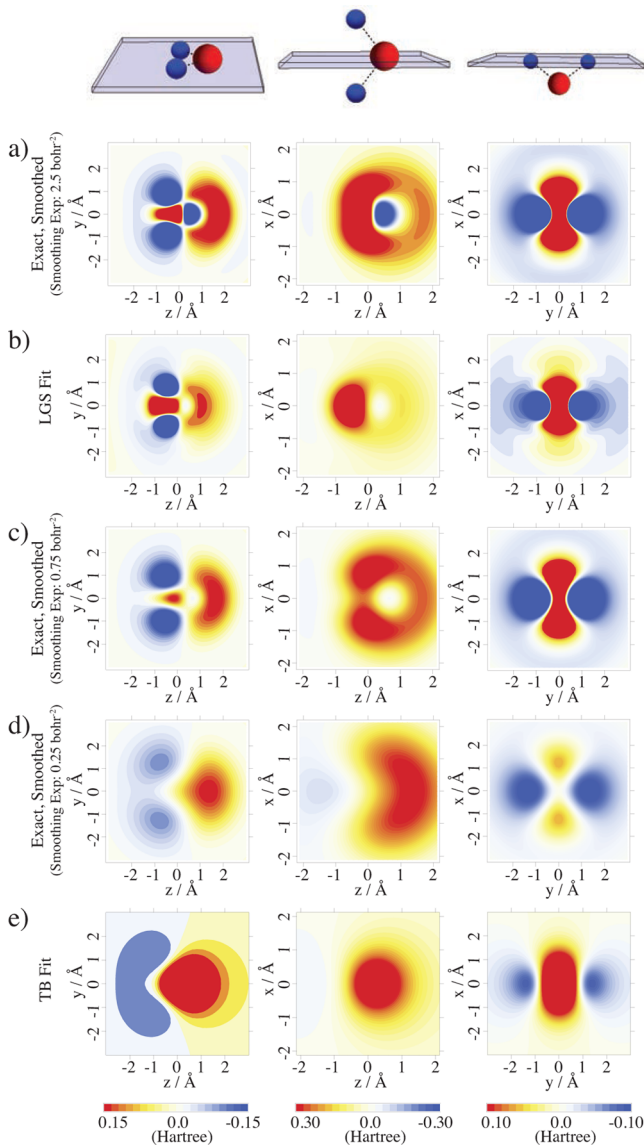


**Figure 2.** Cuts of the full, exact PK electron–water pseudopotential, after smoothing the corresponding pseudorbital with a Gaussian with an exponent of (a)  $2.5 \text{ bohr}^{-2}$ , (c)  $0.75 \text{ bohr}^{-2}$ , (d)  $0.25 \text{ bohr}^{-2}$ , and the (b) LGS and (e) TB fits to the exact (smoothed) pseudopotential. The water molecule lies in the  $y$ - $z$  plane with the dipole pointing along the  $z$ -axis. The O atom is located at  $(0.0 \text{ \AA}, 0.0 \text{ \AA}, 0.11663 \text{ \AA})$ , and the H atoms are located at  $(0.0 \text{ \AA}, 0.76001 \text{ \AA}, -0.46654 \text{ \AA})$  and  $(0.0 \text{ \AA}, -0.76001 \text{ \AA}, -0.46654 \text{ \AA})$ . The left panels show a cut parallel to the molecular  $y$ - $z$  plane with  $x = 0.0 \text{ \AA}$ , the middle panels show a cut perpendicular to the plane of the molecule with  $y = 0.0 \text{ \AA}$ , and the right panels show a cut perpendicular to the molecular plane through the H atoms. The energy scales are in units of Hartree.

calculation of the pseudopotential) at several different spatial resolutions. Part a of Figure 2 shows the pseudopotential in its least adulterated form, while parts c and d of Figure 2 show that the effects of increased smoothing wash out many prominent features of the numerically exact potential, as expected. It is worth noting that, although the LGS potential has been criticized for being overly attractive in the region behind the water O atom,<sup>18</sup> a comparison of the left column of Figure 2a and b shows that the LGS fit actually underestimates the attraction in this region that is present

in the full potential. As the magnitude of the smoothing increases, this attractive feature is essentially completely removed, as is the repulsive feature between the H atoms. What makes the loss of these features interesting is that the TB potential, Figure 2e, bears a striking resemblance to the pseudopotential that has been smoothed to such an extent that most of the features have been washed out. Thus, when evaluating the accuracy of the PK-derived pseudopotentials that have been presented in the literature, one has to compare a potential that has the correct eigenenergy but none of the physical features needed to ensure orthogonality with the electrons in the water MOs (TB), to a potential that has the correct calculated shape but misses the eigenenergy by an amount comparable to  $k_B T$  at room temperature (LGS). This obvious sensitivity to the details of the construction of the pseudopotential make it abundantly clear that a more rigorous, dynamical approach to the construction of a water pseudopotential that responds to a changing environment may be necessary to shed light on the simulation of this system.<sup>23</sup>

The other reason that the LGS non-cavity picture of the hydrated electron has not been well received lies in the fact that it initially appears counterintuitive. Because scientists studying solvated electrons have spent decades developing the idea that closed-shell molecules are intrinsically repelled by excess electrons, the idea of an electron that completely overlaps with these molecules seems to go against our instincts. However, as we show below, the LGS non-cavity electron does not have significant direct overlap between the excess electron's charge density and the interior water molecules; instead, it simply has a different arrangement of the water molecules associated with the charge density. The hydrated electron is a purely quantum mechanical object, capable of significant distortion—contrary to the simple pictures prevalent in the literature, it is not and does not have to behave like a halide ion. In fact, the idea of a non-cavity hydrated electron was explored over 20 years ago by Tuttle and Golden, who compared the absorption spectra of solvated electrons to solvated halide ions and determined that a cavity model for the hydrated electron is inconsistent with the experimental absorption spectra.<sup>24</sup> Instead, they proposed that the spectroscopy of the hydrated electron was more consistent with a solvent–anion complex,<sup>24</sup> a structure which shares many features in common with the LGS simulations.<sup>15</sup> Indeed, moment analysis of the hydrated electron's absorption spectrum tells us that the hydrated electron's charge density has a radius of gyration of  $2.4 \text{ \AA}$ ,<sup>25</sup> but nothing in the spectrum directly indicates whether the water molecules are primarily inside or outside of the charge density.

One might think that the question of the structure of the hydrated electron could be easily settled from fully *ab initio* calculations, but here again, the results have been ambiguous. Most *ab initio* work on the hydrated electron<sup>26</sup> has been performed on small gas-phase water anion clusters.<sup>27,28</sup> The clusters in these studies are usually cold, so the calculated structures are often those of metastable states.<sup>29</sup> In addition to occupying surface states, most water anion cluster studies have shown cavity-type bound states for the excess electron,<sup>29,30</sup> although many also have started with structures that are predisposed to cavity formation rather than to enhanced interior density. The one-electron LGS simulations suggest that the non-cavity structure is stable only in the presence of a sufficient number (of order hundreds) of water molecules so that the interior of the electron is filled and there are several

additional surrounding solvent shells.<sup>15</sup> This places *ab initio* calculations at the limit of what is computationally feasible for density functional theory (DFT) and out of range for more accurate quantum chemistry methods. We note that when the limits are pushed, however, recent cluster calculations based on DFT have shown water density penetrating deep into the electron's center, even for room temperature water (e.g., see Figure 2 of ref 31). And when extending such calculations to bulk liquid water, Uhlig, Marsalek, and Jungwirth (UMJ) have found a hydrated electron that has both cavity and non-cavity characteristics.<sup>32</sup> In UMJ's picture, there is a small central cavity at the center of the hydrated electron's wave function, but over half of the charge density resides among the solvent in a manner reminiscent of that proposed by LGS (Figure 1d).

## ■ EXTENT OF ELECTRON–WATER OVERLAP IN DIFFERENT HYDRATED ELECTRON MODELS

Although *ab initio* calculations support the idea that there can be significant electron–water overlap, we are still left with the conundrum of whether or not the hydrated electron occupies a cavity, encompasses a region of enhanced water density, or has a structure that is some hybrid mixture of the two. To better understand what it really means to have water molecules inside of the hydrated electron and to help determine whether or not a hydrated electron with interior waters is consistent with our physical instincts, we have investigated the amount of electron–water overlap in the SR, TB, LGS, and UMJ models. Once we have a better understanding of what makes these models quantitatively different from each other, we can then focus on how these differences relate to the extent of agreement each of these models has with experiment.

The difficulty in quantifying the extent of electron–water overlap in different models of the hydrated electron is that there is not a unique way to define what is meant by “overlap”. In this work, we define two types of overlap: radial and direct. Radial overlap is what we believe most scientists think about when confronted with the idea of waters interior to the charge density of the hydrated electron; we define the radial overlap  $\Phi$  as the extent to which the average electron charge density at a given distance from the electron's center of mass falls on top of an average number of water molecules that are present at that same distance

$$\Phi = 4\pi \int r^2 g(r) |\Psi(r)|^2 dr \quad (1)$$

where  $r$  is the distance between the electron center of mass (COM) and the O atom on a given water molecule,  $g(r)$  is the  $e^-$ -oxygen radial distribution function, and  $|\Psi(r)|^2$  is the hydrated electron's average charge density. Table 1 shows the

**Table 1. Calculated Percent Radial ( $\Phi$ ) and Direct ( $\Theta$ ) Overlap for the SR, TB, LGS, and UMJ Models<sup>a</sup>**

hydrated electron model	$\Phi$	$\Theta$
SR (cavity)	16.9%	1.0%
TB (cavity)	31.1%	5.7%
LGS (non-cavity)	122%	17.0%
UMJ (hybrid)	63.1%	17.9%

<sup>a</sup>Direct overlap percentages were obtained by averaging over 400 independent configurations, each containing 499 water molecules.

value of  $\Phi$  for each of the four hydrated electron models considered here. Not surprisingly, the two cavity models show relatively little radial overlap of the electron with the nearby waters: the SR model has 16.9% overlap, while the slightly softer TB model has 31.1% radial overlap. It is important to note that even cavity models still have appreciable radial overlap between the electron density and water density; as shown in Figure 1, the “tail” of the electron's wave function extends through the first solvent shell and beyond in both of these models. The LGS non-cavity model, in contrast, has a radial overlap of 122%. This >100% overlap is not unphysical; it arises because the average density of the water molecules inside the hydrated electron's charge density is ~1.22 g/mL,<sup>15</sup> and the electron's wave function has perfect radial overlap with all of the interior waters. Finally, the UMJ hybrid model has 63.1% radial electron–water overlap, roughly halfway between the cavity and non-cavity hydrated electron models.

Although  $\Phi$  tells us a great deal about where the water molecules reside relative to the electron's charge density, the radial overlap does not provide a good measure of how much of the excess electron's charge lies physically on top of the water molecules. Thus, we can define another measure of overlap, the direct overlap  $\Theta$ , as the fraction of the hydrated electron's density that resides inside of spheres centered at the geometric center of mass of each water molecule. This definition depends on the cutoff radius chosen for the sphere,  $r_c$ , with the direct overlap given by

$$\Theta = \left\langle \sum_{i=1}^{n_{\text{mols}}} 4\pi \int_0^{r_c} r_i^2 |\Psi(r_i)|^2 dr_i \right\rangle \quad (2)$$

where the sum runs over each of the water molecules in the simulation and the ensemble average is taken over 400 independent configurations from a >20 ps trajectory. We examined several choices for the value of  $r_c$  and decided that a value of 1.0 Å was the most appropriate, since this size roughly represents the core orbitals of the water molecule: smaller sizes led to negligible values of  $\Theta$ , while larger sizes led to similar values for all the various hydrated electron models. Table 1 shows the calculated direct overlap for the four hydrated electron models considered here with this choice of  $r_c$ : the SR cavity model has a direct overlap of 1.0%, while the TB cavity model has a higher direct overlap of 5.7%. Interestingly, the LGS non-cavity model and the UMJ hybrid model have similar direct overlaps of 17.0 and 17.9%, respectively. These latter values are both very close to the ~20% direct overlap estimated in previous *ab initio* studies.<sup>33,34</sup> The fact that the LGS non-cavity model shows similar amounts of direct overlap to the UMJ and other *ab initio* calculations suggests that a small amount of direct overlap between the excess electron and the water molecules is indeed physically reasonable. Thus, the LGS model is the only MQC model that appears to give a “correct” estimate for the amount of direct electron–water overlap. The various cavity models of the hydrated electron may in fact have too little direct overlap to be physically meaningful, as the amount of overlap they show is much more reminiscent of what is seen for  $\text{Cl}^-(\text{H}_2\text{O})_n$ .<sup>34</sup> And, as we argue further below, the experimental resonance Raman spectrum shows that the hydrated electron cannot have a structure like that of a chloride ion.

Perhaps the most interesting aspect of the overlap data in Table 1 is that there is relatively little direct electron–water

overlap in all of the various hydrated electron models; most of the electron density resides between the water molecules rather than on top of them, even in the LGS non-cavity and UMJ hybrid models. This idea suggests that the descriptor “non-cavity” is not ideal for the LGS model of the hydrated electron; despite the fact that there is no single large cavity to which the electron is confined, the label “non-cavity” does not provide an accurate description as to exactly where the electron resides. In light of our new calculations and reanalysis, we now feel that the LGS hydrated electron is better described as being an “inverse plum pudding” model: the electron is a diffuse ball of charge which occupies multiple interstitial voids present between the water molecules, thus resulting in relatively little direct electron–water overlap (see Figure 3). This picture is reminiscent of a kind of inverse

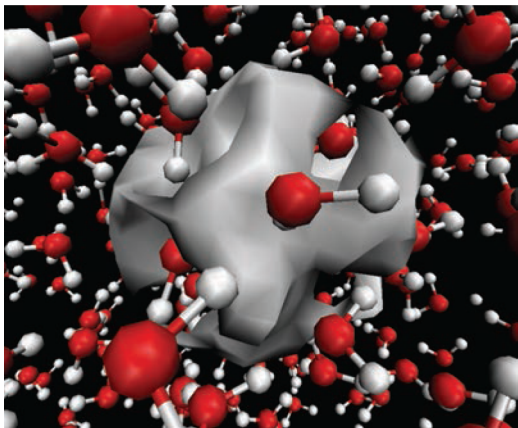


**Figure 3.** LGS water configuration from MD simulation, with exaggerated electron density contours for clearer illustration of the inverse plum pudding effect.

Thompson “plum pudding” model of the atom, which had electrons embedded as “plums” inside a diffuse and spatially extended positive nucleus “pudding”. When viewed this way, it is clear that the LGS and UMJ models of the hydrated electron simply provide an alternative way to arrange the water molecules around the charge density of the excess electron while minimizing the entropic cost of creating a cavity and disrupting liquid water’s strong H-bonding network. In the end, all of the models have the electron density being repelled from the water molecules’ core MOs, in accord with our intuition based on the Pauli exclusion principle. The main difference between the SR, TB, LGS, and UMJ pictures of the hydrated electron is the amount of radial overlap in each model. Thus, we now turn toward understanding how different amounts of radial overlap determine the level of agreement each model has with various experiments.

## ■ COMPARING DIFFERENT HYDRATED ELECTRON MODELS TO EXPERIMENT

Despite the differences in direct and especially radial overlap between the cavity, inverse plum pudding, and hybrid models of the hydrated electron, all of them do an adequate job at predicting basic experimental observables, making it difficult to immediately eliminate any one model. For example, experiment has shown that the hydrated electron has a radius of gyration of  $2.45 \text{ \AA}$ <sup>25</sup> while the SR, TB, and LGS hydrated

electrons have radii of gyration of  $2.25$ ,<sup>35</sup>  $2.42$ ,<sup>11</sup> and  $2.5 \text{ \AA}$ ,<sup>15</sup> respectively (all calculated without the use of Ewald summation, which is known to slightly alter these values<sup>13,19</sup>). The UMJ hydrated electron, on the other hand, shows large fluctuations in the radius of gyration ranging from  $2.4$  to  $4.5 \text{ \AA}$ , with a mean value of  $2.8 \text{ \AA}$ .<sup>32</sup> Thus, even though it has not yet been calculated, the large average value and spread in the radius of gyration of the UMJ model suggests that its optical absorption spectrum would be broadened and red-shifted compared to experiment. Given that the SR, TB, and LGS one-electron models all have roughly the correct radius of gyration, they all predict an optical absorption spectrum of the hydrated electron in reasonable agreement with experiment. The SR cavity model predicts an optical absorption band that is blue-shifted relative to the experimental band by about  $0.7 \text{ eV}$ ,<sup>35</sup> but the absorption band shifts into significantly better agreement with experiment when a mathematical error in the derivation of the SR pseudopotential is corrected.<sup>6</sup> The TB cavity model and the LGS inverse plum pudding model both predict an optical absorption spectrum of the hydrated electron that agrees very well with what is seen experimentally, although the calculated absorption maximum is slightly too blue for the TB model and slightly too red for the LGS model.<sup>11,15</sup>

To further investigate the relationship between different models’ predicted optical absorption spectrum and experiment, Herbert and Jacobson used long-range-corrected time-dependent density functional theory (TD-DFT) to take many-electron effects into account when calculating the absorption spectrum for configurations extracted from various one-electron simulation models of the hydrated electron.<sup>20</sup> What these authors found from their TD-DFT calculations is that the TB model has an absorption spectrum that is in excellent agreement with experiment, whereas the LGS model gives a spectrum that is  $\sim 0.5 \text{ eV}$  too red, and the authors’ polarizable model (which they call PWEP-2) gives a spectrum that is  $\sim 0.4 \text{ eV}$  too blue. Although we understand the impetus for grafting many-electron effects onto calculated properties of the hydrated electron, we note that the configurations used as input for these calculations were still generated from one-electron calculations (which themselves are based on pseudopotentials that are derived either empirically or at the Hartree–Fock level of theory), so it is not clear that the calculations themselves are internally consistent. Moreover, because of the computational expense involved, these authors were able to explicitly include only a few tens of the closest water molecules to the electron’s COM in their TD-DFT calculations. This limitation puts the LGS model at a distinct disadvantage, since the calculation includes mostly the interior waters, and not the large number of exterior waters whose polarization helps to bind the electron and reduce the radius of gyration to what is seen experimentally, explaining why the spectrum calculated this way is overly red-shifted.

Thus, it seems that, no matter what the level of theory, any calculation that gives an electron with a radius of gyration close to  $2.45 \text{ \AA}$  will give an absorption spectrum that is reasonably consistent with experiment, whether or not the electron has interior water molecules. It is for this reason why we turned to the experimentally known temperature dependence of the hydrated electron’s absorption spectrum to distinguish between these different models. Experiments have shown that the maximum of the hydrated electron’s optical absorption spectrum undergoes a roughly linear red-shift with

increasing temperature (2.2 meV/K), even when the water density is held constant.<sup>36,37</sup> We recently calculated the optical absorption spectra of the hydrated electron at fixed density as a function of temperature using the SR, TB, and LGS models (see Figure 3 of ref 17). We found that the LGS inverse plum pudding model was able to capture the red-shift with increasing temperature, but the calculated slope was about a factor of 2.4 larger than experiment. In contrast, the SR and TB cavity models showed no spectral shift with changing temperature at constant density, giving a slope of zero or an effective error of infinity relative to experiment. Thus, the calculated temperature dependence suggests that an inverse plum pudding picture is more consistent with experiment than a cavity picture of the hydrated electron. We attribute this agreement between the inverse plum pudding picture and experiment to the attractive features found in the LGS pseudopotential that were effectively smoothed away in the TB and other potentials.<sup>17</sup>

Another important feature of the hydrated electron's optical absorption spectrum is whether it is homogeneously or inhomogeneously broadened. For systems like the hydrated electron, which have the bulk of their absorption between a ground state and three quasi-degenerate and orthogonal excited states, polarized hole-burning experiments can be used to determine the degree of homogeneous broadening.<sup>38</sup> Early calculations based on the SR cavity model of the polarized hole-burning experiment predicted a clear polarized hole-burning signature and a homogeneous line width that is about half of the full line width.<sup>39</sup> Subsequent calculations using different cavity models, however, have been less clear about what the polarized hole-burning experiment should show for the hydrated electron.<sup>13,40,41</sup> The LGS model predicts a homogeneously broadened line; in this inverse plum pudding picture, librational motions of the interior waters cause the orientations of the three excited states to quickly rotate, so that absorption to each of the three states has the same width as the full spectrum.<sup>15</sup> The experimental results of the polarized hole-burning experiment on the hydrated electron also have not been clear-cut. Early experiments showed a clear polarized hole-burning signature,<sup>42</sup> suggesting an inhomogeneously broadened line, but the preponderance of later experiments have found no polarized hole-burning and thus conclude that the spectrum is homogeneously broadened.<sup>43–45</sup> Similar experiments have also concluded that the absorption spectrum of the solvated electron in methanol is homogeneously broadened.<sup>43</sup> Recently, Doan and Schwartz discovered that there is a clear polarized hole-burning signature for solvated electrons in liquid acetonitrile; the spectroscopy indicates that the homogeneous line width is about half of the full line width.<sup>46</sup> Doan and Schwartz have argued that solvated electrons in acetonitrile must therefore occupy cavities and that, by extension, hydrated electrons (as well as solvated electrons in methanol and other solvents that are similar in polarity to acetonitrile but in which the solvated electron's absorption is homogeneously broadened) do not. Moreover, these authors have speculated that H-bonding solvents are less likely to form cavity solvated electrons than non-H-bonding solvents, because the free energetic cost to break up the H-bond network is simply too high to form a cavity.<sup>46</sup>

Beyond the optical absorption spectrum, probably the best experimental indicator of the structure of the hydrated electron comes from resonance Raman spectroscopy, which provides a direct measure of the changes in the local H-

bonding environment associated with electronic excitation of the electron. Tauber and Mathies,<sup>47–49</sup> as well as Tahara and co-workers,<sup>50</sup> have measured the resonance Raman spectrum of the hydrated electron, and found that the O–H stretching band is red-shifted and broadened compared to that of bulk liquid water. We recently extended a semiclassical theory developed by Skinner and co-workers, which relates the O–H stretching frequency of a condensed-phase water molecule to the local electric field experienced by the water H atom,<sup>51–53</sup> to calculate the resonance Raman spectrum of the hydrated electron with the SR, TB, and LGS models, as shown in Figure 4.<sup>17</sup> We found that both of the cavity models predict

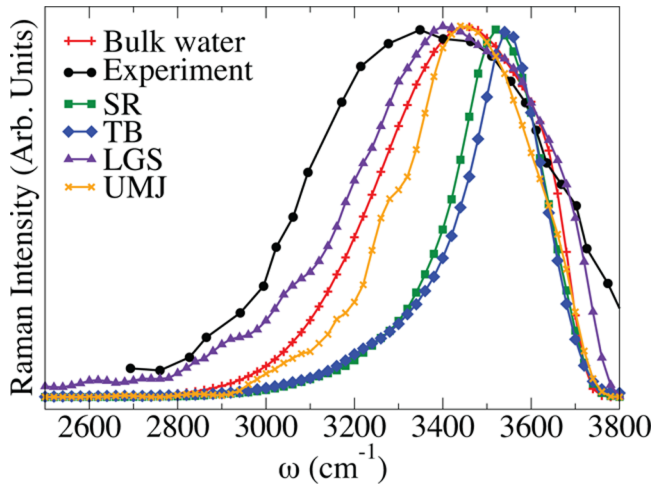


**Figure 4.** The experimental resonance Raman spectrum of the hydrated electron (black circles/curve, from ref 49) compared to the calculated Raman spectrum for bulk SPC/Flex water (red plus signs/curve), the force-weighted calculated resonance Raman spectrum of the SR (green squares/curve), TB (blue diamonds/curve), and LGS (purple triangles/curve) models, and the 4 Å cutoff calculated resonance Raman spectrum of the UMJ (orange crosses/curve) model of the hydrated electron. Both the SR and TB models produce Raman spectra that are blue-shifted and narrowed compared to the bulk spectrum, in stark contrast to the experiment, while the LGS model correctly predicts that the resonance Raman spectrum of the hydrated electron should be both broader and red-shifted relative to that of bulk water. The UMJ hybrid model's spectrum is broader and more red-shifted than the SR and TB cavity model spectra but is still unable to capture the broadening and red-shift compared to the pure spectrum that is seen experimentally.

resonance Raman spectra that are in qualitative disagreement with experiment: the cavity models predict O–H stretching bands that are narrower and blue-shifted relative to that of bulk water. In fact, the resonance Raman spectra of the SR and TB hydrated electrons are very reminiscent of the larger halides dissolved in water.<sup>54,55</sup> Thus, the local breaking of water's H-bonding structure that is seen in cavity models of the hydrated electron is inconsistent with the experimental resonance Raman spectrum. In contrast, the LGS inverse plum pudding model is able to correctly capture the red-shift and broadening of the O–H stretch seen experimentally. This is because the water molecules inside of the LGS electron density experience a variety of environments and orientations, leading to a broader spectrum than seen in pure water, and the higher density of water inside the electron leads to stronger H-bonding that helps contribute to the red-shift.<sup>17</sup>

To better understand how the hybrid picture of the hydrated electron compares to experiment, we also have calculated the resonance Raman spectrum for the UMJ model. We first verified that the electric field distribution for *ab initio* water molecules calculated with the same level of theory used by UMJ is nearly identical to that for the classical SPC water model, so that the calculated Raman spectrum for bulk DFT water is essentially identical to that shown for bulk SPC water in Figure 4. Unfortunately, the DFT calculation performed by UMJ does not give information on the electronic excited states that are needed to calculate the displacement of the water O–H stretches upon excitation. Consequently, we used the approximation outlined in ref 17, where, instead of using the force-weighting method to calculate the contribution of each water molecule to the resonance Raman spectrum, we took advantage of the fact that equally weighting all molecules within 4 Å of the electron's center of mass provides a good approximation to the true resonance Raman spectrum. The orange crosses and curve in Figure 4 show the results, indicating that the UMJ model of the hydrated electron predicts a broader and more red-shifted O–H stretch than the cavity models but is still unable to capture the experimental red-shift and broadening of the O–H stretch compared to that of the pure water spectrum. This is because the presence of even a small central cavity breaks the local H-bond structure of the water, producing a qualitatively incorrect predicted Raman spectrum.

## CONCLUSIONS

In this Feature Article, we have reflected on the nature of the structure of the hydrated electron. Although there has been a lot of resistance to the idea that there may be water molecules in the interior of the electron's charge density, we have seen that, in fact, there is relatively little direct overlap of the electron's wave function with the interior water molecules. Considering this idea in combination with the fact that *ab initio* calculations also suggest that there can be interior waters with a small amount of direct overlap, it seems that inverse plum pudding and hybrid structures must be considered with at least equal weight alongside the more traditional cavity models. Even the traditional cavity models have a significant amount of their charge density outside the first solvation shell, while the LGS inverse plum pudding model still has a small deficit of water density right at the electron's center of mass (cf. Figure 1 and Table 1), so distinguishing cavity vs inverse plum pudding models involves a continuum more than a two-state approach. It is important to note that none of the models discussed here show perfect quantitative agreement with experiment, so the exact average structure of the hydrated electron is still unknown. Thus, the question we are asking in many ways is a semantic one: do we want our zeroth order picture for the structure of the hydrated electron to have a significant number of interior water molecules, or not? And how should we weigh the evidence from different one-electron and *ab initio* simulations to help us decide?

All of the models considered here provide good agreement with the experimental absorption spectrum and most of the pump–probe transient absorption experiments<sup>25,42,43,56</sup> that have been performed on the hydrated electron.<sup>13,39–41,57</sup> However, given the variety of models that produce such similar predictions on this front, the question of whether or not there are interior waters depends on the details of the potential between a water molecule and the excess electron.

Figure 2 shows that, based on quantum chemistry calculations, there should be attractive regions (beyond the simple Coulomb attraction of the excess electron to the positively charged H atoms) in this interaction potential, at least at the one-electron level. These attractive features are entirely ignored in the TB and SR cavity models and are included to some extent in the LGS model, but the “true” potential, if such a thing exists, appears to be right at the tipping point where interior waters become stable.<sup>16,18</sup> *Ab initio* calculations aimed at this problem are also at their limits, as it is a challenge to find functionals and basis sets that can describe the structure of an excess unpaired electron whose density resides almost entirely between the hundreds of water molecules that are needed to provide a converged structure. Thus, the best we can do at this point is examine how well each model can predict observables for the few experiments where the subtle differences between the various models can be discerned.

Perhaps the most sensitive measure of the balance between the attractive and repulsive terms in the electron–water interaction comes in the temperature dependence of the hydrated electron's optical properties. So far, none of the various cavity models have been able to reproduce the known red-shift of the experimental spectrum with increasing temperature at constant density, whereas the LGS inverse plum pudding model is in qualitative agreement with experiment, although it somewhat overestimates the magnitude of the shift. The LGS model is also the only one that is able to capture both the red-shift and broadening of the resonance Raman O–H stretch spectrum of the hydrated electron relative to that of bulk water. Models that break the local H-bond structure of the water molecules near the electron, such as the cavity and hybrid models explored here, provide qualitatively incorrect predictions of the shape of the resonance Raman O–H stretching band (cf. Figure 4). Thus, even though the LGS model does not provide quantitative agreement with experiment, it appears that its inverse plum pudding picture provides the most reasonable general agreement with experiment.

Given that there still is not consensus on the nature of the hydrated electron's structure, where can we go from here in terms of trying to further distinguish the various models against experiment? One example of potential interest is the behavior of the hydrated electron at interfaces. Our intuition says that cavity and inverse plum pudding models of the hydrated electron should make dramatically different predictions as to whether or not the electron prefers to reside at the interface. For example, one might expect a cavity hydrated electron, which prefers to expel water molecules from its center, to preferentially localize at an interface, much like the larger halides.<sup>58–60</sup> Placing a cavity electron at the interface would limit the structure breaking effects of the hydrated electron, and make it easier for such an electron to locally expel the water molecules. On the other hand, a hydrated electron that contains a significant number of interior water molecules likely prefers to avoid the interface. This is because it would be difficult for an inverse plum pudding electron to have an increased interior water density at an interface where water molecules are scarce. Although there is not an abundance of experimental data on the behavior of hydrated electrons at interfaces, there is some indirect evidence that hydrated electrons prefer the bulk to the interface. For example, interface-sensitive second harmonic

generation (SHG) experiments show no signals from samples in which hydrated electrons have been generated in the interior.<sup>61</sup> Moreover, pulse radiolysis experiments in silica pore glasses with ~1 nm channel diameters have found no changes in the hydrated electron's absorption spectrum relative to that in bulk water,<sup>62</sup> again suggesting that the electron is avoiding the interface. There is some simulation work exploring the behavior of cavity electrons at air/water interfaces,<sup>30,63</sup> and we are currently working on making a detailed comparison between the behavior of cavity and inverse plum pictures of the hydrated electron that should provide yet another direct confrontation with experiment. Overall, even though the inverse plum pudding picture of the hydrated electron seems unconventional at first, the idea certainly has merit in that this model has proven to be more consistent with experiment than the traditional cavity picture. We look forward to future simulations and experiments that will continue to build our understanding of the elusive hydrated electron.

## AUTHOR INFORMATION

### Corresponding Author

\*E-mail: schwartz@chem.ucla.edu.

### Notes

The authors declare no competing financial interest.

### Biographies



Jennifer Ryan Casey received her B.S. degree in Chemistry from the California State University of Long Beach in 2007. She is currently working on her Ph.D. in Physical Chemistry under the guidance of Benjamin J. Schwartz at the University of California, Los Angeles. Her research interests include exploring the behavior of free electrons in condensed phase systems and investigating solvation effects.



Argyris Kahros received his B.S. in Chemistry from UC Berkeley in 2005 and is currently working towards a Ph.D. in Physical Chemistry from UCLA under the tutelage of Benjamin J. Schwartz. His research interests include how the presence of a solvent affects the bonding electronic structure of a molecular solute and the rigorous development of dynamical, molecular pseudopotentials for use in mixed quantum/classical molecular dynamics simulations.



Benjamin J. Schwartz received his Bachelor's degree in Physics and Chemistry from the University of Michigan in 1986 and his Ph.D. in Experimental Physical Chemistry from UC Berkeley in 1992. After carrying out postdoctoral work in theoretical physical chemistry at the University of Texas, Austin (1993–1995 with Peter J. Rossky) and experimental physics at UC Santa Barbara (1995–1996, with 2000 Nobel Laureate Alan Heeger), he joined the faculty at UCLA in 1997. He was promoted to Associate Professor with tenure in 2002 and Full Professor in 2004. Prof. Schwartz' research interests include quantum non-adiabatic processes in condensed phases studied from both theoretical and ultrafast spectroscopic points of view as well as studies of the fundamental processes underlying the operation of conjugated polymer-based solar cells.

## ACKNOWLEDGMENTS

This work was supported by the National Science Foundation under Grant Nos. CHE-0908548 and CHE-1212951. We thank Pavel Jungwirth and his co-workers for providing the configurations needed to calculate the Raman spectrum of the UMJ model, and for a critical reading of this manuscript. We also thank William Glover for insightful discussions about this work.

## REFERENCES

- (1) Turi, L.; Rossky, P. J. Theoretical Studies of Spectroscopy and Dynamics of Hydrated Electrons. *Chem. Rev.* **2012**, *112*, 5641–5674.
- (2) Ogg, R. A. Physical Interaction of Electrons with Liquid Dielectric Media. The Properties of Metal-Ammonia Solutions. *Phys. Rev.* **1946**, *69*, 668–669.
- (3) Schnitker, J.; Rossky, P. J. Quantum Simulation Study of the Hydrated Electron. *J. Chem. Phys.* **1987**, *86*, 3471–3485.
- (4) Wallqvist, A.; Martyna, G.; Berne, B. J. Behavior of the Hydrated Electron at Different Temperatures: Structure and Absorption Spectrum. *J. Phys. Chem.* **1988**, *92*, 1721–1730.
- (5) Barnett, R. N.; Landman, U.; Cleveland, C. L. Electron Localization in Water Clusters. II. Surface and Internal States. *J. Chem. Phys.* **1988**, *88*, 4429–4447.
- (6) Larsen, R. E.; Glover, W. J.; Schwartz, B. J. Comment on "An Electron-Water Pseudopotential for Condensed Phase Simulations". *J. Chem. Phys.* **2009**, *131*, 037101/1–037101/2.

- (7) Schnitker, J.; Rossky, P. J. An Electron-Water Pseudopotential for Condensed Phase Simulations. *J. Phys. Chem.* **1987**, *86*, 3462–3469.
- (8) Schnitker, J.; Rossky, P. J. The Hydrated Electron: Quantum Simulation of Structure, Spectroscopy, and Dynamics. *J. Phys. Chem.* **1988**, *92*, 4277–4285.
- (9) Kevan, L. Solvated Electron Structure in Glassy Matrices. *Acc. Chem. Res.* **1981**, *14*, 138–145.
- (10) Turi, L.; Gaigeot, M.-P.; Levy, N.; Borgis, D. Analytical Investigations of an Electron-Water Pseudopotential. 1. Exact Calculation on a Model. *J. Chem. Phys.* **2001**, *114*, 7805–7815.
- (11) Turi, L.; Borgis, D. Analytical Investigations of an Electron-Water Molecule Pseudopotential. 2. Development of a New Pair Potential and Molecular Dynamics Simulations. *J. Chem. Phys.* **2002**, *117*, 6186–6195.
- (12) Jacobson, L. D.; Williams, C. F.; Herbert, J. M. The Static-Exchange Electron-Water Pseudopotential, in Conjecture with a Polarizable Water Model: A new Hamiltonian for Hydrated-Electron Simulations. *J. Chem. Phys.* **2009**, *130*, 124115/1–124115/18.
- (13) Jacobson, L. D.; Herbert, J. M. A One-Electron Model for the Aqueous Electron That Includes Many-Body Polarization: Bulk Equilibrium Structure, Vertical Electron Binding Energy, and Optical Absorption Spectrum. *J. Chem. Phys.* **2010**, *133*, 154506/1–154506/19.
- (14) Voora, V. K.; Ding, J.; Sommerfeld, T.; Jordan, K. D. A Self-Consistent Polarization Potential Model for Describing Excess Electrons Interacting with Water Clusters. *J. Phys. Chem. B* **2013**, *117*, 4365–4370.
- (15) Larsen, R. E.; Glover, W. J.; Schwartz, B. J. Does the Hydrated Electron Occupy a Cavity? *Science* **2010**, *329*, 65–69.
- (16) Larsen, R. E.; Glover, W. J.; Schwartz, B. J. Response to comments on “Does the Hydrated Electron Occupy a Cavity?”. *Science* **2011**, *331*, 1387e.
- (17) Casey, J. R.; Larsen, R. E.; Schwartz, B. J. Resonance Raman and Temperature-Dependent Electronic Absorption Spectra of Cavity and Noncavity Models of the Hydrated Electron. *Proc. Natl. Acad. Sci. U.S.A.* **2013**, *110*, 2712–2717.
- (18) Turi, L.; Madarasz, A. Comment on “Does the Hydrated Electron Occupy a Cavity?”. *Science* **2011**, *331*, 1387c.
- (19) Jacobson, L. D.; Herbert, J. M. Comment on “Does the Hydrated Electron Occupy a Cavity?”. *Science* **2011**, *331*, 1387d.
- (20) Herbert, J. M.; Jacobson, L. D. Sturcture of the Aqueous Electron: Assessment of One-Electron Pseudopotential Models in Comparision to Experimetal Data and Time-Dependent Density Functional Theory. *J. Phys. Chem. A* **2011**, *115*, 14470–14483.
- (21) Phillips, J. C.; Kleinman, L. New Method for Calculating Wave Functions for Crystals and Molecules. *Phys. Rev.* **1959**, *116*, 287–294.
- (22) Smallwood, C. J.; Larsen, R. E.; Glover, W. J.; Schwartz, B. J. A Computationally Efficient Exact Pseudopotential Method 1. Analytical Reformulation of Phillips-Kleinman Theory. *J. Chem. Phys.* **2006**, *125*, 074102/1–074102/9.
- (23) Kahros, A.; Schwartz, B. J. Going Beyond the Frozen Core Approximation: Development of Coordinate-Dependent Pseudopotentials and Applicaiton to  $\text{Na}_2^+$ . *J. Chem. Phys.* **2013**, *138*, 054110/1–054110/9.
- (24) Tuttle, T. R.; Golden, S. Solvated Electrons: What is Solvated? *J. Phys. Chem.* **1991**, *95*, 5725–5736.
- (25) Bartels, D. M. Moment Analysis of Hydrated Electron Cluster Spectra: Surface or Internal States? *J. Chem. Phys.* **2001**, *115*, 4404–4405.
- (26) Boero, M.; Parrinello, M.; Terakura, K.; Ikeshoji, T.; Liew, C. C. First-Principles Molecular-Dynamics Simulations of a Hydrated Electron in Normal and Supercritical Water. *Phys. Rev. Lett.* **2003**, *90*, 226403/1–226403/4.
- (27) Herbert, J. M.; Head-Gordon, M. First-Principles, Quantum-Mechanical Simulations of Electron Solvation by a Water Cluster. *Proc. Natl. Acad. Sci. U.S.A.* **2006**, *103*, 14282–14287.
- (28) Marsalek, O.; Uhlig, F.; Jungwirth, P. Electrons in Cold Water Clusters: An Ab Initio Molecular Dynamics Study of Localization and Metastable States. *J. Phys. Chem. C* **2010**, *114*, 20489–20495.
- (29) Marsalek, O.; Uhlig, F.; Frigato, T.; and Pavel Jungwirth, B. S. Dynamics of Electron Localization in Warm Versus Cold Clusters. *Phys. Rev. Lett.* **2010**, *105*, 043002/1–043002/4.
- (30) Madarasz, A.; Rossky, P. J.; Turi, L. Excess Electron Relaxation Dynamics at Water/Air Interface. *J. Chem. Phys.* **2007**, *126*, 234707/1–234707/11.
- (31) Marsalek, O.; Uhlig, F.; Vandevondele, J.; Jungwirth, P. Structure, Dynamics, and Reactivity of Hydrated Electrons by Ab Initio Molecular Dynamics. *Acc. Chem. Res.* **2012**, *45*, 23–32.
- (32) Uhlig, F.; Marsalek, O.; Jungwirth, P. Unraveling the Complex Nature of the Hydrated Electron. *J. Phys. Chem. Lett.* **2012**, *3*, 3071–3075.
- (33) Shkrob, I. A.; Glover, W. J.; Larsen, R. E.; Schwartz, B. J. The Structure of the Hydrated Electron. Part 2. A Mixed Quantum/Classical Molecular Dynamics Embedded Cluster Density Functional Theory: Single-Excitation Configuration Interaction Study. *J. Phys. Chem. A* **2007**, *111*, 5232–5243.
- (34) Herbert, J. M.; Head-Gordon, M. Charge Penetration and the Origin of Large O–H Vibrational Red-Shifts in Hydrated-Electron Clusters,  $(\text{H}_2\text{O})_n^-$ . *J. Am. Chem. Soc.* **2006**, *128*, 13932–13939.
- (35) Schnitker, J.; Motakabbir, K.; Rossky, P. J.; Friesner, R. A Priori Calculation of the Optical-Absorption Spectrum of the Hydrated Electron. *Phys. Rev. Lett.* **1988**, *60*, 456–459.
- (36) Bartels, D. M.; Takahashi, K.; Cline, J. A.; Marin, T. W.; Jonah, C. D. Pulse Radiolysis of Supercritical Water. 3. Spectrum and Thermodynamics of the Hydrated Electron. *J. Phys. Chem. A* **2005**, *109*, 1299–1307.
- (37) Du, Y.; Price, E.; Bartels, D. M. Solvated Electron Spectrum in Supercooled Water and Ice. *Chem. Phys. Lett.* **2007**, *438*, 234–237.
- (38) Yu, J.; Berg, M. Local Anisotropy and Structural and Phonon Dynamics of Permanganate ( $\text{MnO}_4^-$ ) in Glassy and Liquid Lithium Chloride Hexahydrate by Ultrafast Transient Hole Burning. *J. Phys. Chem.* **1993**, *97*, 1758–1764.
- (39) Schwartz, B. J.; Rossky, P. J. Hydrated Electrons as a Probe of Local Anisotropy: Simulations of Ultrafast Polarization-Dependent Spectra Hole Burning. *Phys. Rev. Lett.* **1994**, *72*, 3282–3285.
- (40) Shkrob, I. A. Pump-Probe Polarized Transient Hole-Burning (PTHB) Dynamics of the Hydrated Electron Revised. *Chem. Phys. Lett.* **2008**, *467*, 84–87.
- (41) Bratos, S.; Leicknam, J. C. Pump-Probe Absorption Anisotropy of the Hydrated Electron. A Theory. *Chem. Phys. Lett.* **1998**, *291*, 496–500.
- (42) Reid, P. J.; Silva, C.; Walhout, P. K.; Barbara, P. F. Femtosecond Absorption Anisotropy of the Aqueous Solvated Electron. *Chem. Phys. Lett.* **1994**, *228*, 658–664.
- (43) Cavanagh, M. C.; Martini, I. B.; Schwartz, B. J. Revisiting the Pump-Probe Polarized Transient Hole-Burning of the Hydrated Electron: Is its Absorption Spectrum Inhomogeneously Broadened? *Chem. Phys. Lett.* **2004**, *396*, 359–366.
- (44) Assei, M.; Laenen, R.; Laubereau, A. Dynamics of Excited Solvated Electrons in Aqueous Solution Monitored with Femtosecond-Time and Polarizaiton Resolution. *J. Phys. Chem. A* **1998**, *102*, 2256–2262.
- (45) Baltuska, A.; Emde, M. F.; Pshenichnikov, M. S.; Wiersma, D. A. Early-Time Dynamics of the Photoexcited Hydrated Electron. *J. Phys. Chem. A* **1999**, *103*, 10065–10082.
- (46) Doan, S. C.; Schwartz, B. J. Nature of Excess Electrons in Polar Fluids: Anion-Solvated Electron Equilibrium and Polarized Hole-Burning in Liquid Acetonitrile. *J. Phys. Chem. Lett.* **2013**, *4*, 1471–1476.
- (47) Tauber, M. J.; Mathies, R. A. Fluorescence and Resonance Raman Spectra of the Aqueous Solvated Electron. *J. Phys. Chem. A* **2001**, *105*, 10952–10960.
- (48) Tauber, M. J.; Mathies, R. A. Resonace Raman spectra and vibronic analysis of the aqueous solvated electron. *Chem. Phys. Lett.* **2002**, *354*, 518–526.

- (49) Tauber, M. J.; Mathies, R. A. Structure of the Aqueous Solvated Electron from Resonance Raman Spectroscopy: Lessons from Isotopic Mixtures. *J. Am. Chem. Soc.* **2003**, *125*, 1394–1402.
- (50) Mizuno, M.; Tahara, T. Novel Resonance Raman Enhancement of Local Structure Around Solvated Electrons in Water. *J. Phys. Chem. A* **2001**, *105*, 8823–8826.
- (51) Corcelli, S. A.; Lawrence, C. P.; Skinner, J. L. Combined Electronic Structure/Molecular Dynamics Approach for Ultrafast Spectroscopy of Dilute HOD in Liquid H<sub>2</sub>O and D<sub>2</sub>O. *J. Chem. Phys.* **2004**, *120*, 8107–8117.
- (52) Corcelli, S. A.; Skinner, J. L. Infrared and Raman Line Shapes of Dilute HOD in Liquid H<sub>2</sub>O and D<sub>2</sub>O from 10 to 90°C. *J. Phys. Chem. A* **2005**, *109*, 6154–6165.
- (53) Auer, B.; Kamar, R.; Schmidt, J. R.; Skinner, J. L. Hydrogen Bonding and Raman, IR, and 2D-IR Spectroscopy of Dilute HOD in Liquid D<sub>2</sub>O. *Proc. Natl. Acad. Sci. U.S.A.* **2007**, *104*, 14215–14220.
- (54) Smith, J. D.; Saykally, R. J.; Geissler, P. L. The Effects of Dissolved Halide Anions on Hydrogen Bonding in Liquid Water. *J. Am. Chem. Soc.* **2007**, *129*, 13847–13856.
- (55) Perera, P. N.; Browder, B.; Ben-Amotz, D. Perturbations of Water by Alkali Halide Ions Measured Using Multivariate Raman Curve Resolution. *J. Phys. Chem. B* **2009**, *113*, 1805–1809.
- (56) Yokoyama, K.; Silva, C.; Son, D. H.; Walhout, P. K.; Barbara, P. F. Detailed Investigation of the Femtosecond Pump-Probe Spectroscopy of the Hydrated Electron. *J. Phys. Chem. A* **1998**, *102*, 6957–6966.
- (57) Rossky, P. J.; Schwartz, B. J. Pump-probe Spectroscopy of the Hydrated Electron: A Quantum Molecular Dynamics Simulation. *J. Chem. Phys.* **1994**, *101*, 6917–6926.
- (58) Dang, L. X. Characterization of Water Octamer, Nanomer, Decamer, and Iodide-Water Interactions Using Molecular Dynamics Techniques. *J. Chem. Phys.* **1999**, *110*, 1526–1532.
- (59) Jungwirth, P.; Tobias, D. J. Ions at the Air/Water Interface. *J. Phys. Chem. B* **2002**, *106*, 6361–6373.
- (60) Rodriguez, J.; Laria, D. Electronic States at the Water/Air Interface. *J. Phys. Chem. B* **2005**, *109*, 6473–6478.
- (61) Sagar, D. M.; Bain, C. D.; Verlet, J. R. R. Hydrated Electrons at the Air/Water Interface. *J. Am. Chem. Soc.* **2010**, *132*, 6917–6919.
- (62) Musat, R. M.; Cook, A. R.; Renault, J.-P.; Crowell, R. A. Nanosecond Pulse Radiolysis of Nanoconfined Water. *J. Phys. Chem. C* **2012**, *116*, 13104–13110.
- (63) Uhlig, F.; Marsalek, O.; Jungwirth, P. Electron at the Surface of Water: Dehydration or Not? *J. Phys. Chem. Lett.* **2013**, *4*, 338–343.